

A decorative graphic consisting of several overlapping, semi-transparent spheres in shades of blue, green, and yellow. The spheres are arranged in a cluster, with some overlapping others, creating a sense of depth and movement. The background is a dark blue grid pattern.

Mechano-activated channels: PIEZO

Main characteristics

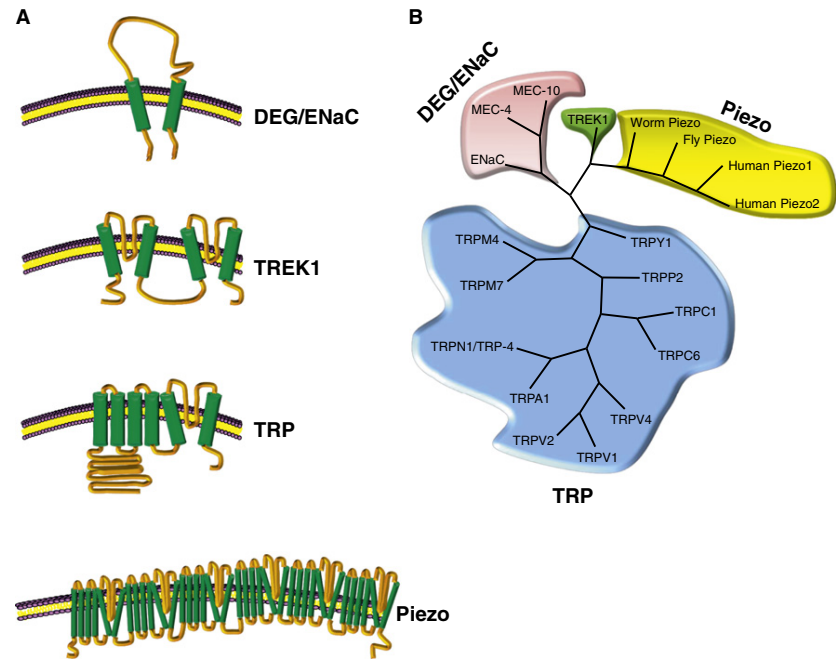
- 🌐 Mechanosensitive channels has been detected in nearly every organism. These channels are directly gated by forces to convert mechanical stimuli into electrical signals and thus function as the force transducer in mechanosensory transduction
- 🌐 Mechanosensitive channels open very rapidly with short latency, usually less than 5 milliseconds, which makes it unlikely that second messengers are involved in channel gating.

Main characteristics

- 🌐 It is generally believed that the three common mechanical sensory modalities — touch, hearing and proprioception — are mediated by mechanosensitive channels that are directly gated by forces.
- 🌐 The molecular identities of these channels, however, remain largely elusive, particularly in mammals. A new study by Coste et al., published recently in Science, has now shed light on this enigma.

Mechano-sensitive channels in eukaryotes

the biophysical properties of mechanosensitive channels recorded from different cell types show large variation, suggesting that the molecular nature of mechanosensitive channels is highly heterogeneous



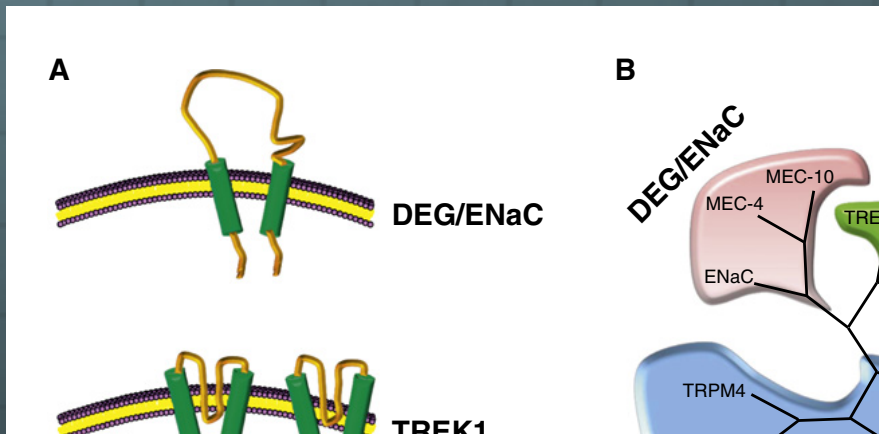
Current Biology

Figure 1. Mechanosensitive channels in eukaryotes.

(A) Schematics of mechanosensitive channels in eukaryotes. Only one subunit is shown for each channel. The membrane topology of Piezo is unclear, and one possibility is shown here. (B) A dendrogram plot of different classes of putative mechanosensitive channels. In the case of TRP family channels, only those that have been implicated in mechanosensation are included, amongst which TRPN1 is the only TRP protein that has been demonstrated to function as a mechanosensitive channel that is mechanically gated [12].

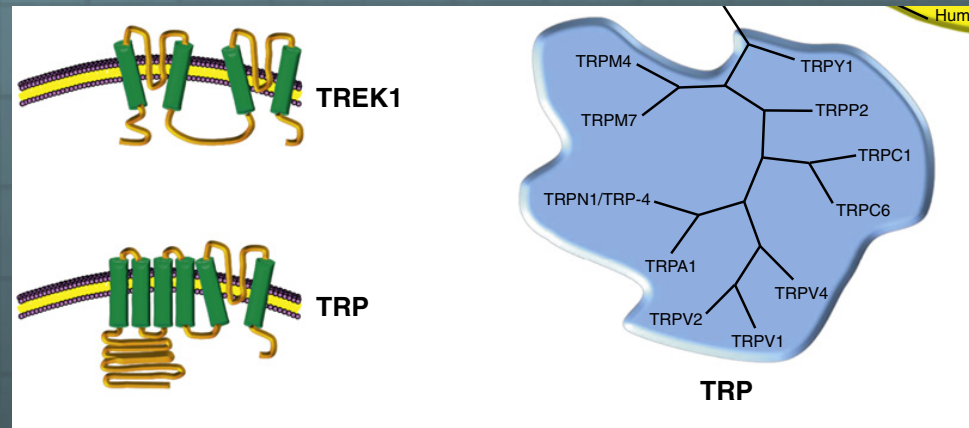
Mechano-sensitive channels in eukaryotes

- The first breakthrough came from studies in the genetic model organism *Caenorhabditis elegans*. Using genetic and electrophysiological approaches, Chalfie and colleagues have identified a mechanosensitive channel complex comprising MEC-4, MEC-10, MEC-2 and MEC-6 that senses gentle body touch in *C. elegans*. MEC-4 and MEC-10 form the channel pore.



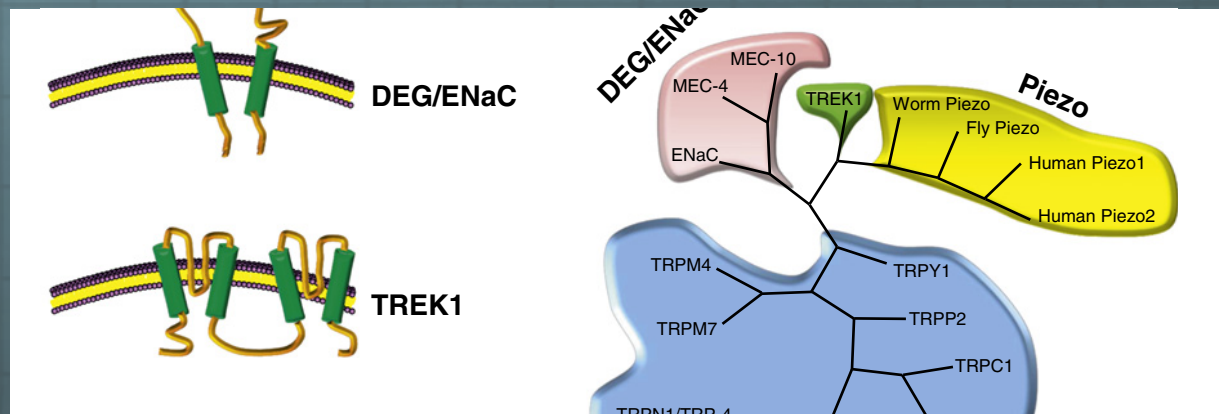
- MEC-4 and MEC-10 belong to the ENaC/DEG family of sodium channels that are conserved from worms to humans

Mechano-sensitive channels in eukaryotes



- 🌐 TRP family channels have recently emerged as another class of leading candidates for mechanosensitive channels.

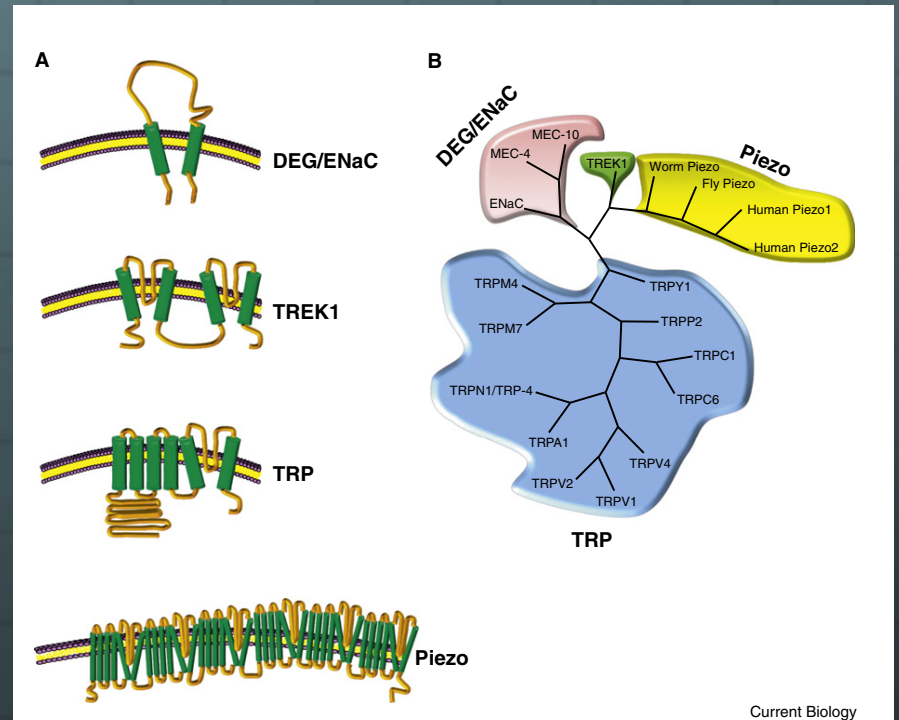
Mechano-sensitive channels in eukaryotes



- 🌐 A second, but not mutually exclusive, possibility is that mechanosensitive channels in mammals are encoded by completely different types of genes. Indeed, the two-pore-domain K⁺ channel TREK1 has been reported to form a mechanosensitive channel in mammals, but, given that the opening of this K⁺ channel hyperpolarizes rather than depolarizes a neuron, it cannot be the primary channel mediating touch, hearing and proprioception in mammals.

Mechano-sensitive channels in eukaryotes

In 2010, Patapoutian and colleagues have identified a novel class of mechanosensitive channels in mammals.



Current Biology

Figure 1. Mechanosensitive channels in eukaryotes.

(A) Schematics of mechanosensitive channels in eukaryotes. Only one subunit is shown for each channel. The membrane topology of Piezo is unclear, and one possibility is shown here. (B) A dendrogram plot of different classes of putative mechanosensitive channels. In the case of TRP family channels, only those that have been implicated in mechanosensation are included, amongst which TRPN1 is the only TRP protein that has been demonstrated to function as a mechanosensitive channel that is mechanically gated [12].

Piezo1 and Piezo2 Are Essential Components of Distinct Mechanically Activated Cation Channels

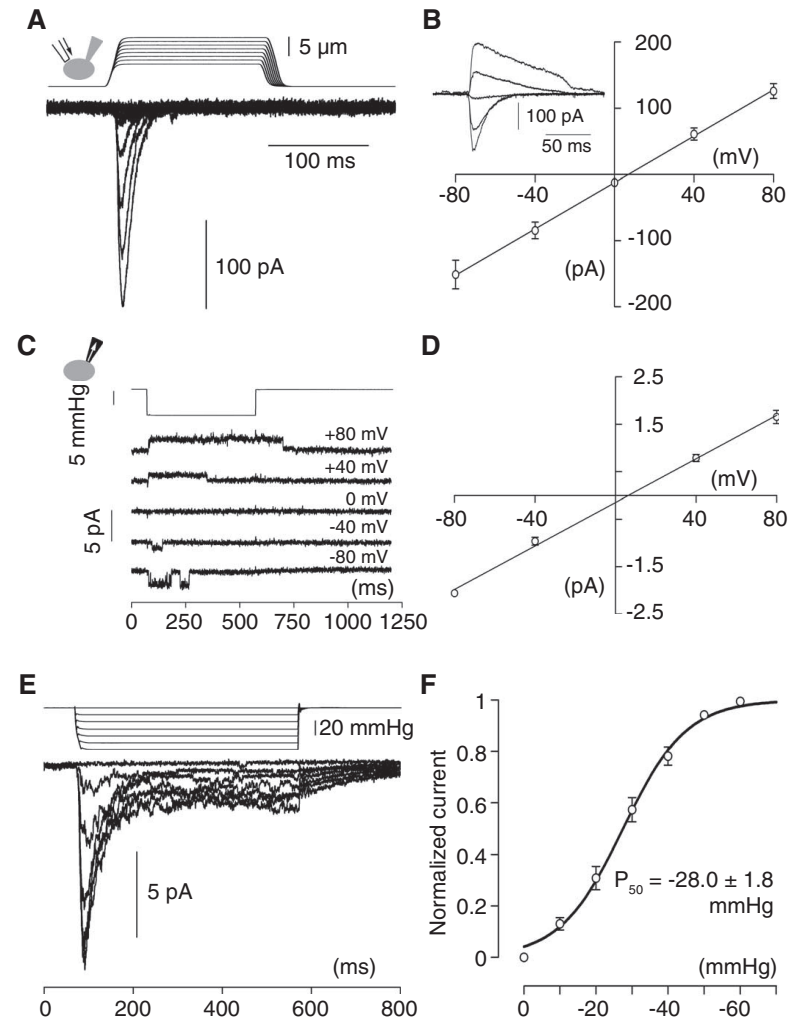
Bertrand Coste,¹ Jayanti Mathur,² Manuela Schmidt,¹ Taryn J. Earley,¹ Sanjeev Ranade,¹ Matt J. Petrus,² Adrienne E. Dubin,¹ Ardem Patapoutian^{1,2*}

www.sciencemag.org SCIENCE VOL 330 1 OCTOBER 2010

55

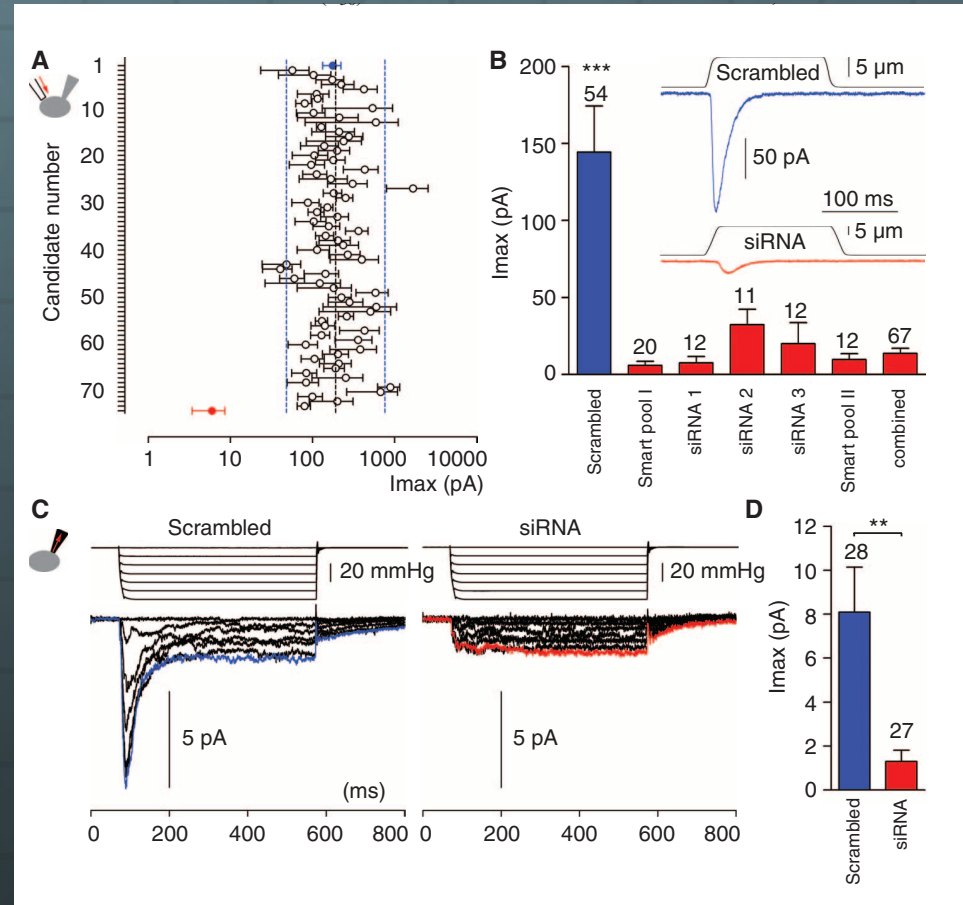
The authors used the mouse neuroblastoma cell line Neuro2A (N2A), which expresses endogenous rapidly-adapting mechanosensitive channels. Two protocols were used to evoke mechanosensitive currents — membrane touch and membrane stretch.

Fig. 1. MA currents in N2A cells. **(A)** Representative traces of MA inward currents expressed in N2A cells. Cells were subjected to a series of mechanical steps of 1- μm movements of a stimulation pipette (inset illustration, arrow) in the whole-cell patch configuration at a holding potential of -80 mV . **(B)** Average current-voltage relationships of MA currents in N2A cells ($n = 11$ cells). (Inset) Representative MA currents evoked at holding potentials ranging from -80 to $+40\text{ mV}$ (applied 0.7 s before the mechanical step). **(C)** Single-channel currents (cell attached patch configuration) induced by means of negative pressure with a pipette (inset illustration, arrow) at holding potentials ranging from -80 to $+80\text{ mV}$ in a N2A cell. **(D)** Average current-voltage relationships of stretch-activated single channels in N2A cells ($n = 4$ cells, mean \pm SEM). Single-channel conductance was calculated from the slope of the linear regression line of each cell, giving $\gamma = 22.9 \pm 1.4\text{ pS}$ (mean \pm SEM). Single-channel amplitude was determined as the amplitude difference in Gaussian fits of full-trace histograms. **(E)** Representative currents (averaged traces) induced by means of negative pipette pressure (0 to -60 mmHg , $\Delta 10\text{ mmHg}$) in a N2A cell. **(F)** Normalized current-pressure relationship of stretch-activated currents at -80 mV fitted with a Boltzmann equation ($n = 21$ cells). P_{50} is the average value of P_{50} values from individual cells.




To generate a list of candidate MA ion channels in N2A, we searched for transcripts that are enriched in N2A cells using Affymetrix microarrays. We selected proteins predicted to span the membrane at least two times (a characteristic shared by all ion channels). We prioritized this list by picking either known cation channels or proteins with unknown function. We tested each candidate (table S1) using small interfering RNA (siRNA) knockdown in N2A cells, measuring MA currents during piezo-driven pressure stimulation in the whole-cell mode.

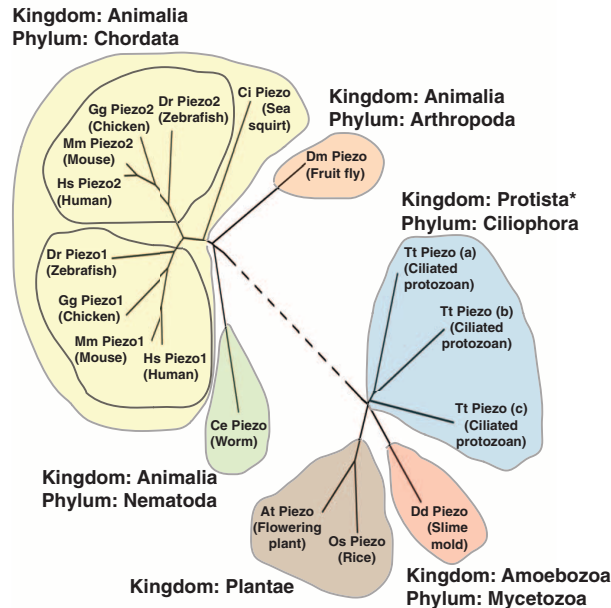
Knockdown of Fam38 (Family with sequence similarity 38) caused a pronounced decrease of MA currents



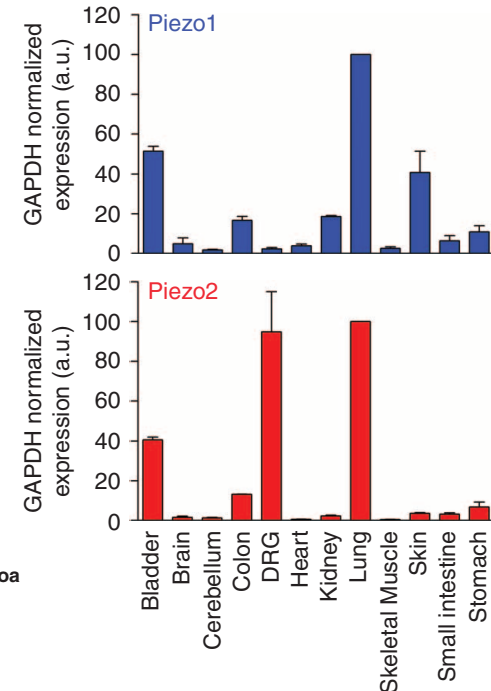
Given that Fam38A encodes a protein required for the expression of ion channels activated by pressure, **we named this gene Piezo1, from the Greek "πίεση" (piesi), meaning pressure.**

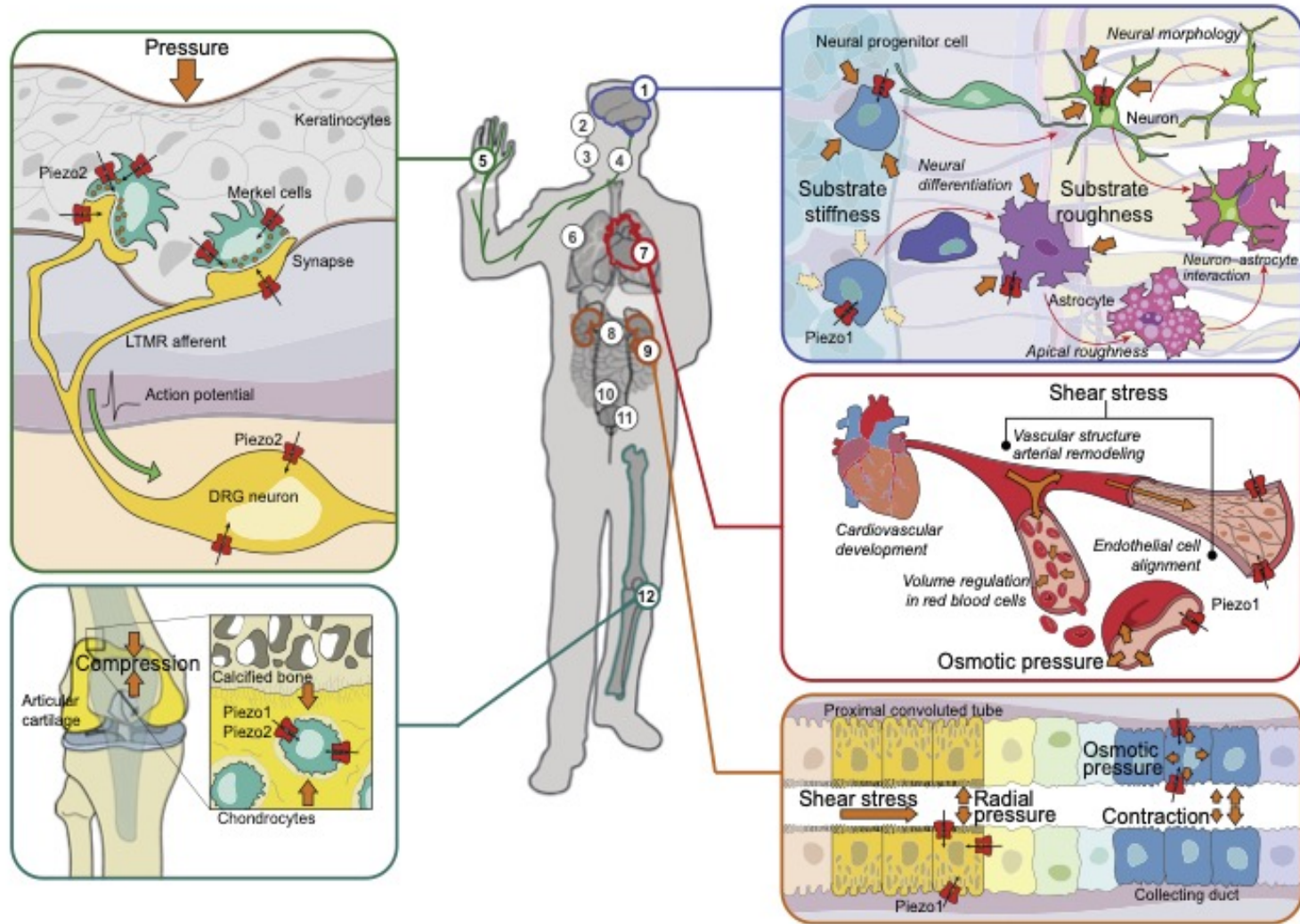
 Many animal, plant, and other eukaryotic species contain a single Piezo. Vertebrates have two members, Piezo1 (Fam38A) and Piezo2 (Fam38B)

A



B

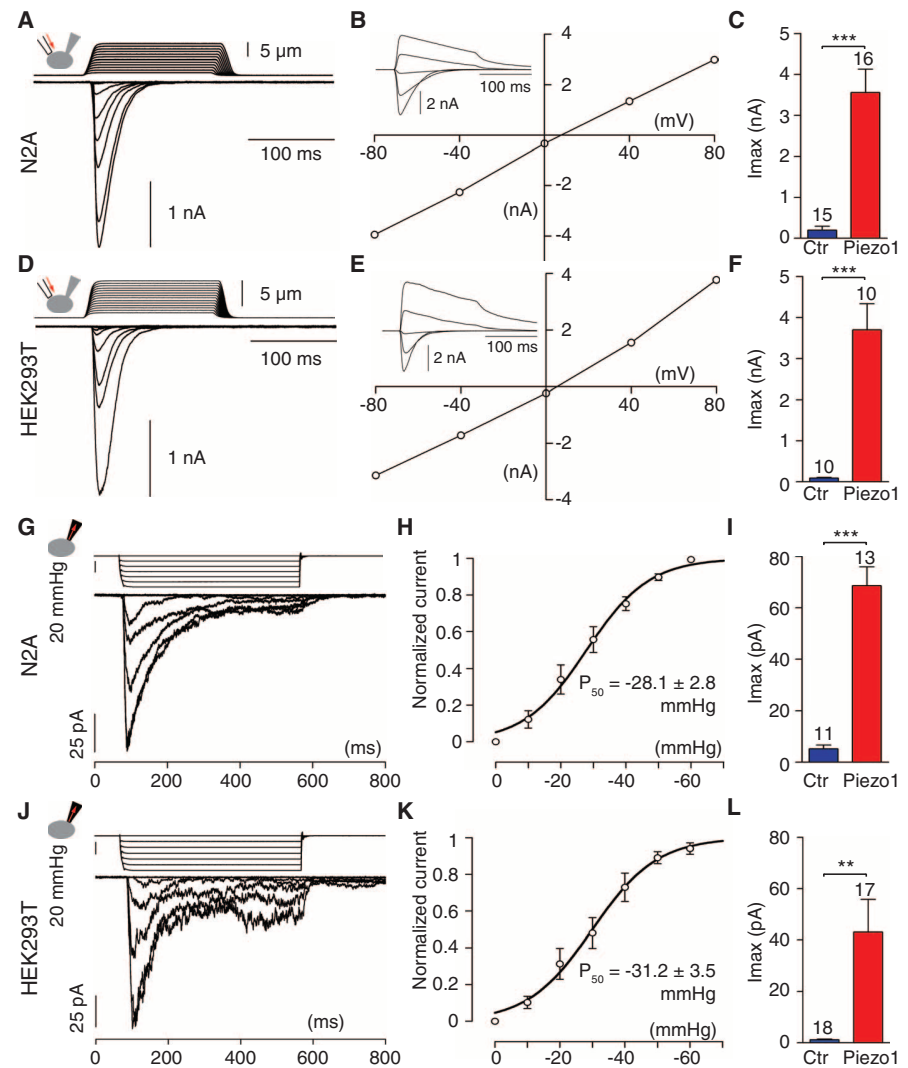





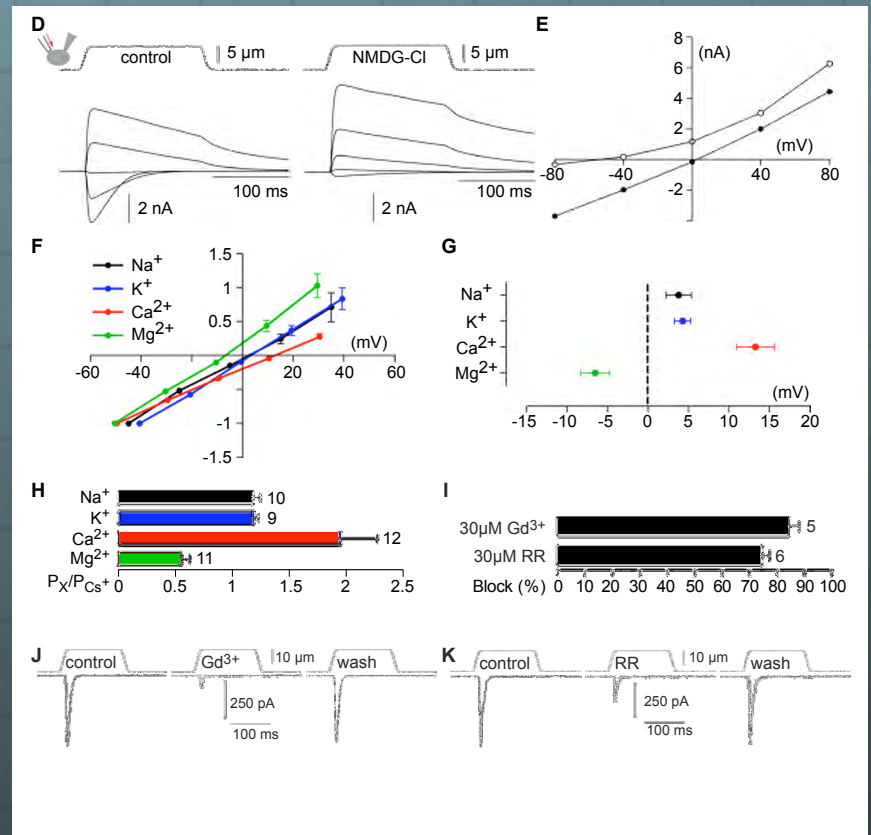
Piezo1 induces MA currents in various cell types

We cloned full-length Piezo1 from N2A cells into the pIRES2-enhanced green fluorescent protein (EGFP) vector. We recorded MA currents from GFP-positive cells in the whole cell mode 12 to 48 hours after transfection. Piezo1 but not mock-transfected cells showed large MA currents in N2A, human embryonic kidney (HEK) 293 T

The threshold of activation and the time constant for inactivation of MA currents elicited in Piezo1-overexpressing cells was similar in all three cell lines tested



 We characterized the ionic selectivity of MA currents in cells overexpressing Piezo1. Substituting the nonpermeant cation NMDG (N-methyl-d-glucamine) in the extracellular bathing solution suppressed inward MA currents, demonstrating that this channel conducts cations



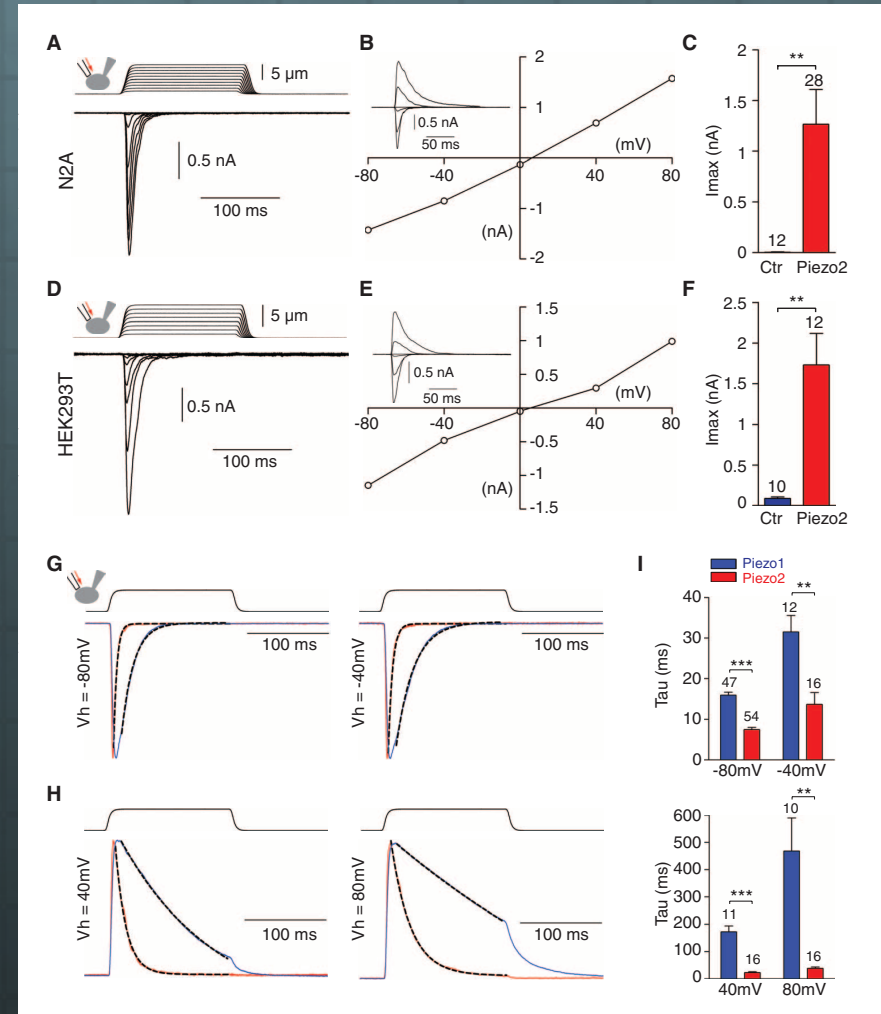
We further examined ionic selectivity by recording with CsCl-only internal solutions and various cations in the bath. Na⁺, K⁺, Ca²⁺ and Mg²⁺ all permeated, with a slight preference for Ca²⁺. Moreover, 30 μM of ruthenium red and gadolinium, which are known blockers of many cationic MA current, blocked 74.6 ± 2.5% (n = 6 cells) and 84.3 ± 3.8% (n = 5 cells) of Piezo1 induced MA current, respectively (fig. S4, I to K).

MA currents in cells overexpressing Piezo2.

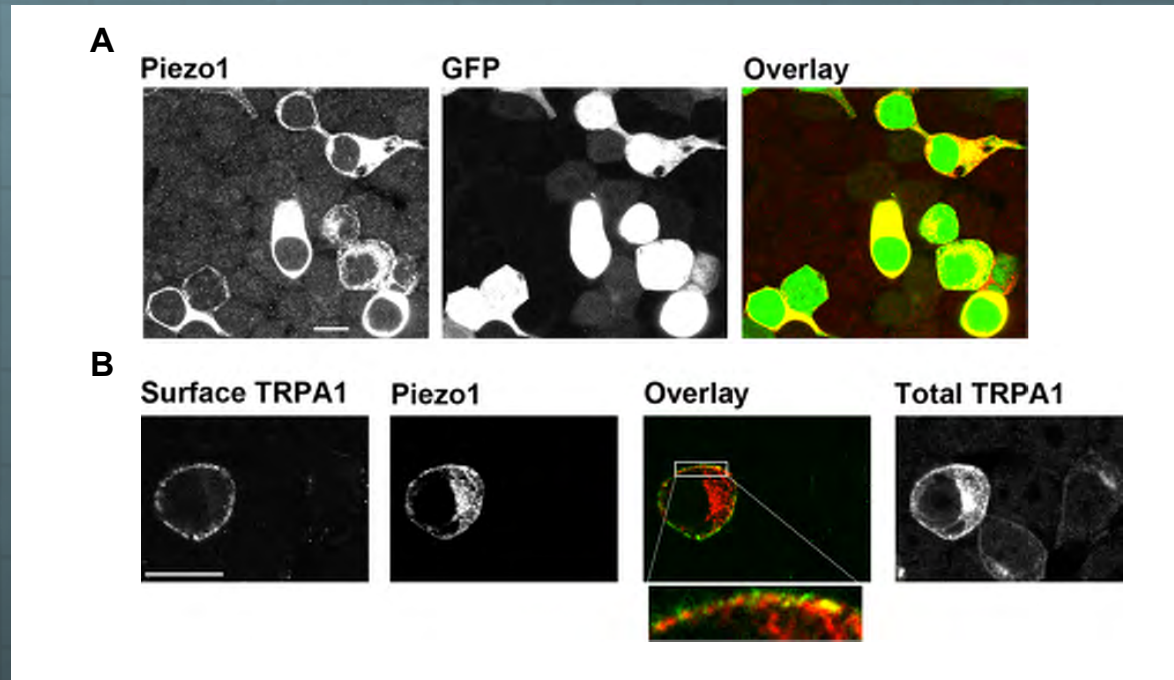
We cloned full-length Piezo2 from DRG neurons. N2A and HEK293T cells transfected with Piezo2 and gene-encoding GFP showed large MA currents (Fig. 5, A to F).

The N2A cells were also cotransfected with Piezo1 siRNA to suppress endogenous MA currents.

The kinetics of inactivation of Piezo2-dependent MA currents were faster than Piezo1-dependent MA currents, both for inward (Fig. 5G) and outward (Fig. 5H) currents, and at all holding potentials tested (Fig. 5I). **Therefore, Piezo1 and Piezo2 confer distinct channel properties**



Piezo1 is detected at the plasma membrane

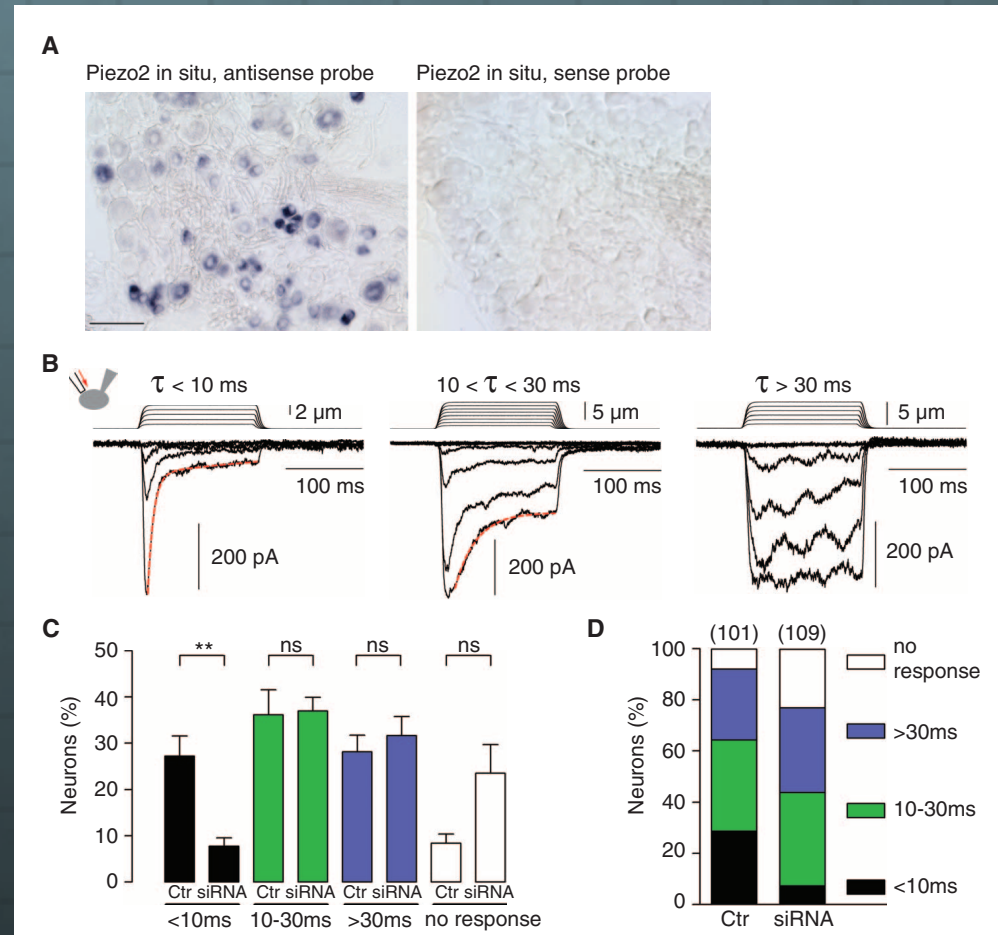


- 🌐 In cells transfected with Piezo1 and TRPA1—an ion channel known to be expressed at the plasma membrane—we observed some overlap of Piezo1 staining with that of TRPA1 on the cell surface, although most Piezo1 and TRPA1 was present inside the cell (fig. S6B). Thus, Piezo1 protein can be localized at or near the plasma membrane

Requirement of Piezo2 for rapidly adapting MA currents in DRG neurons

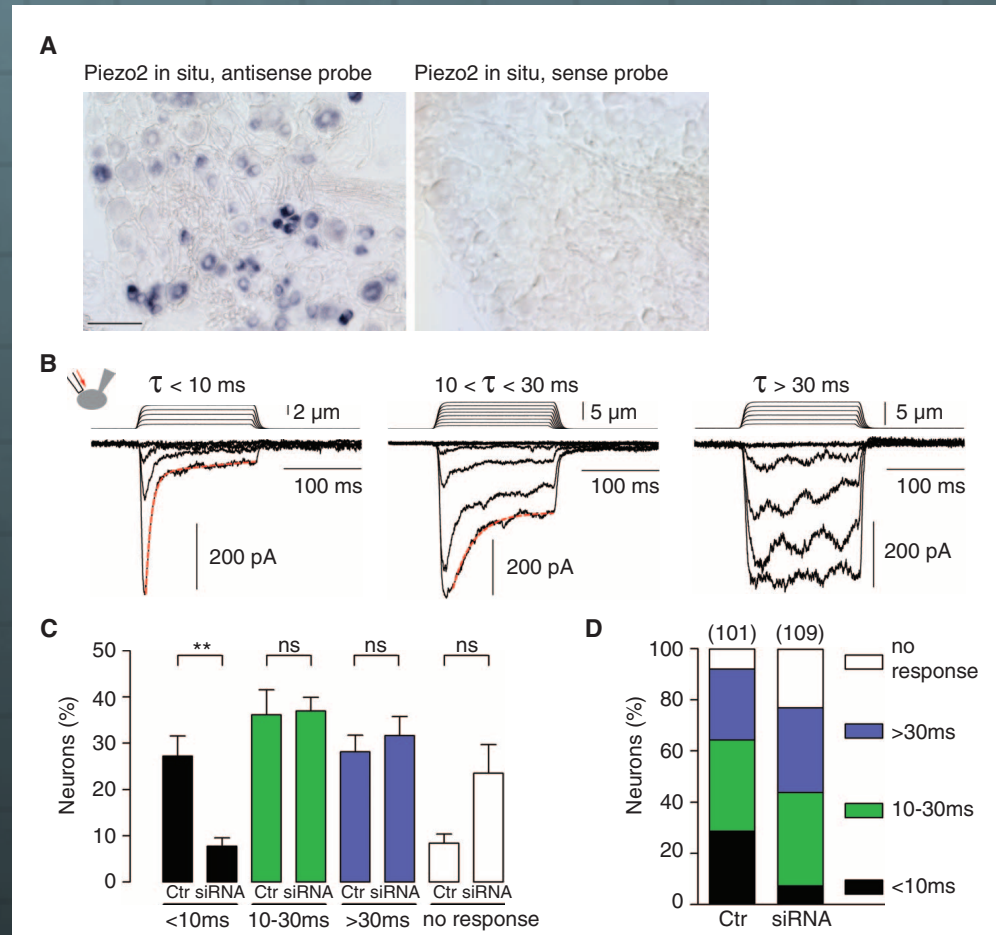
To characterize Piezo2 expression within the heterogeneous population of neurons and glial cells of the DRGs, we performed **in situ hybridization** on adult mouse DRG sections (Fig. 6A)

We observed **Piezo2** mRNA expression **in 20% of DRG neurons**



Requirement of Piezo2 for rapidly adapting MA currents in DRG neurons

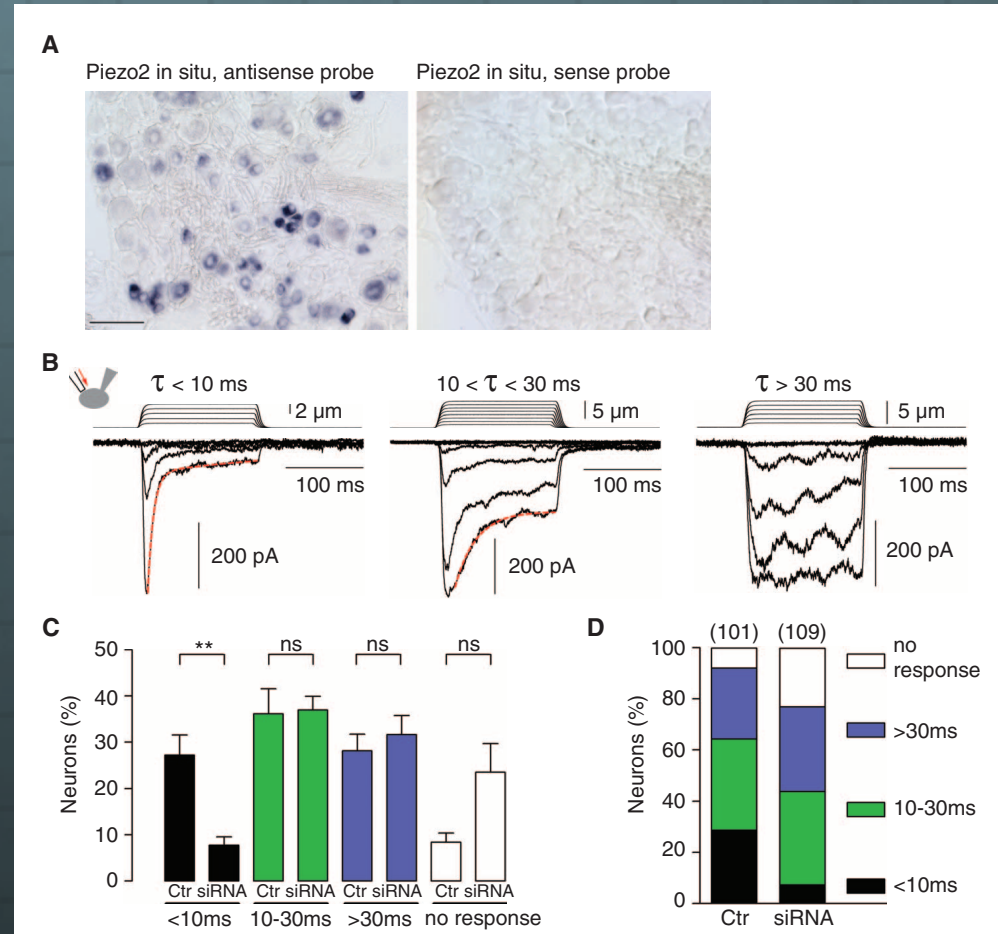
We recorded **whole-cell MA currents from DRG neurons** transfected with GFP and either scrambled or Piezo2 siRNA (n = 101 neurons for scrambled and n = 109 neurons for Piezo2 siRNA). We grouped the recorded MA currents according to their inactivation kinetics (Fig. 6B). We defined four different classes of neurons on the basis of t_{inac} distribution in scrambled siRNA transfected cells



Requirement of Piezo2 for rapidly adapting MA currents in DRG neurons

The proportion of neurons expressing MA currents with τ inact < 10ms was specifically and significantly reduced in neurons transfected with Piezo2 siRNA as compared with that of neurons transfected with scrambled siRNA (Fig. 6C).

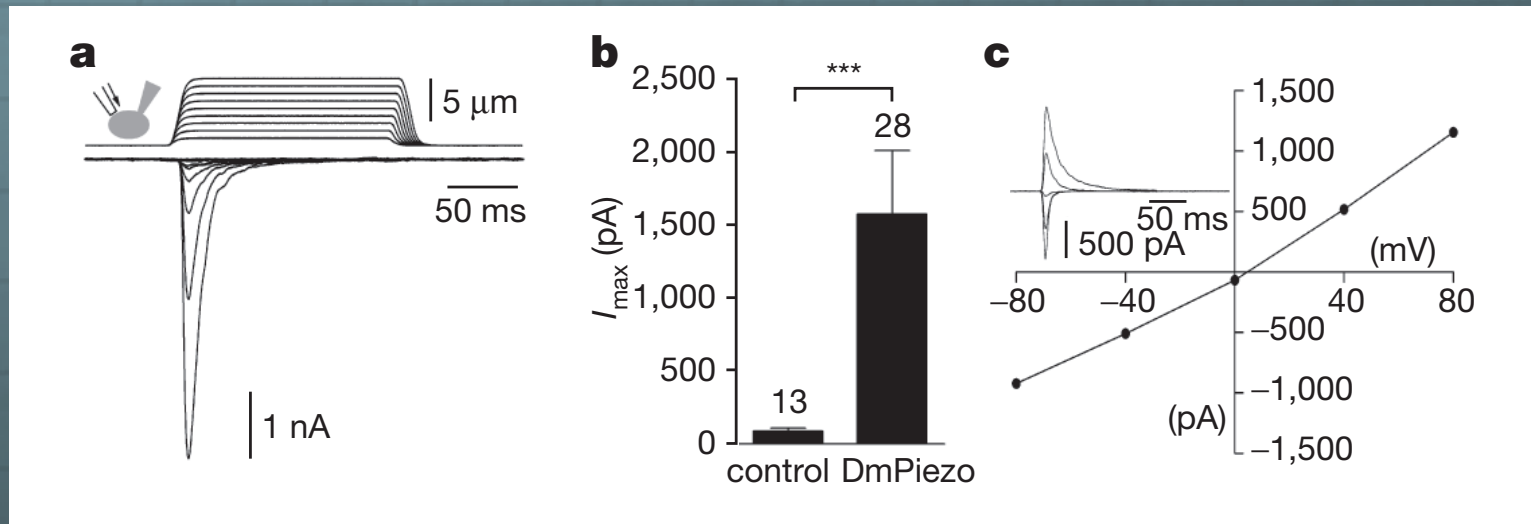
28.7% of scrambled siRNA-transfected neurons had τ inact < 10 ms, compared with 7.3% in Piezo2 siRNA-transfected neurons (Fig. 6D)



Mechanosensitivity of DmPiezo

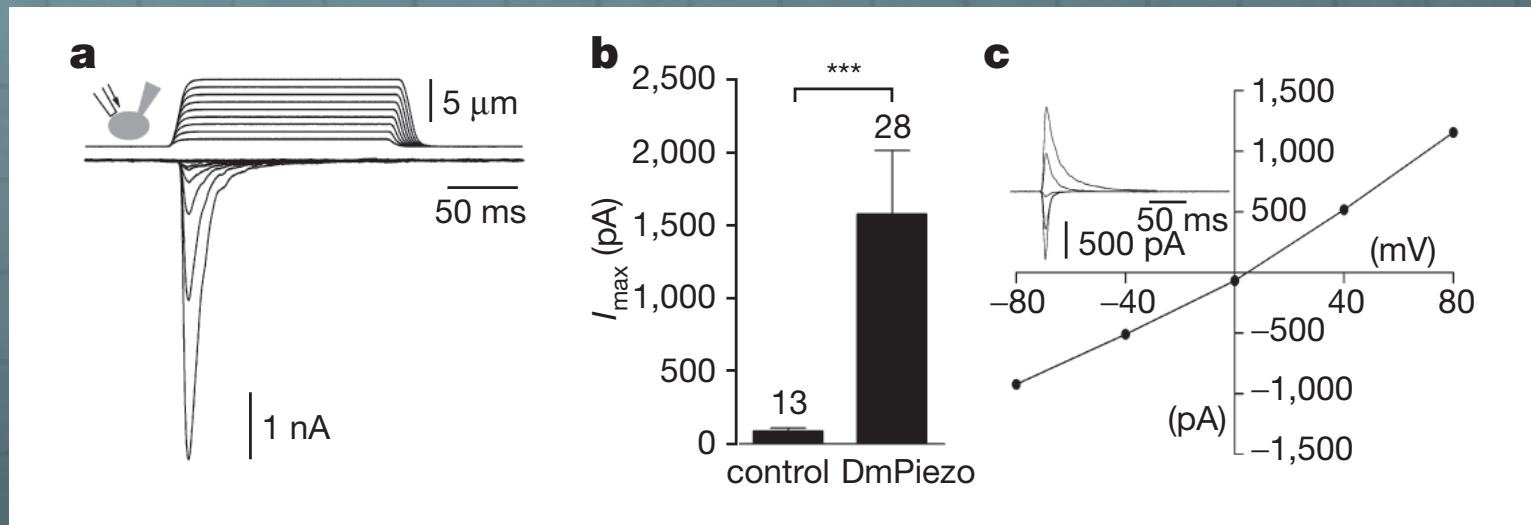
- 🌐 We focused on the apparently single member of **D. melanogaster Piezo (DmPiezo)**, as this invertebrate species is widely used to study mechanotransduction using genetic approaches.
- 🌐 We **cloned the full-length DmPiezo** complementary DNA into pIRES2-EGFP vector.

Mechanosensitivity of DmPiezo



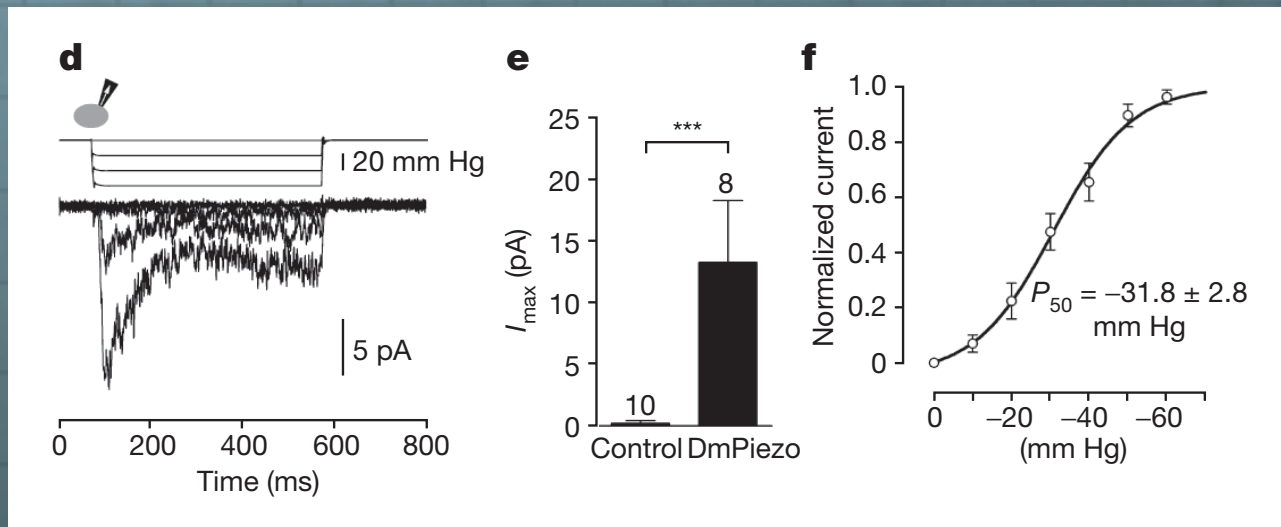
We recorded mechanically activated currents from fluorescent HEK293T cells expressing DmPiezo-pIRES2-EGFP by applying force to the cell surface while monitoring transmembrane currents at constant voltage using patch-clamp recordings in the whole-cell configuration

Mechanosensitivity of DmPiezo



- 🌐 DmPiezo, but not mock-transfected cells, showed large mechanically activated currents (Fig. 1a, b).
- 🌐 Similar to its mammalian counterparts, DmPiezo mechanically activated currents are characterized by a linear current–voltage (I–V) relationship with a reversal potential around 0mV, consistent with it mediating a non-selective cationic conductance (Fig. 1c).

Mechanosensitivity of DmPiezo

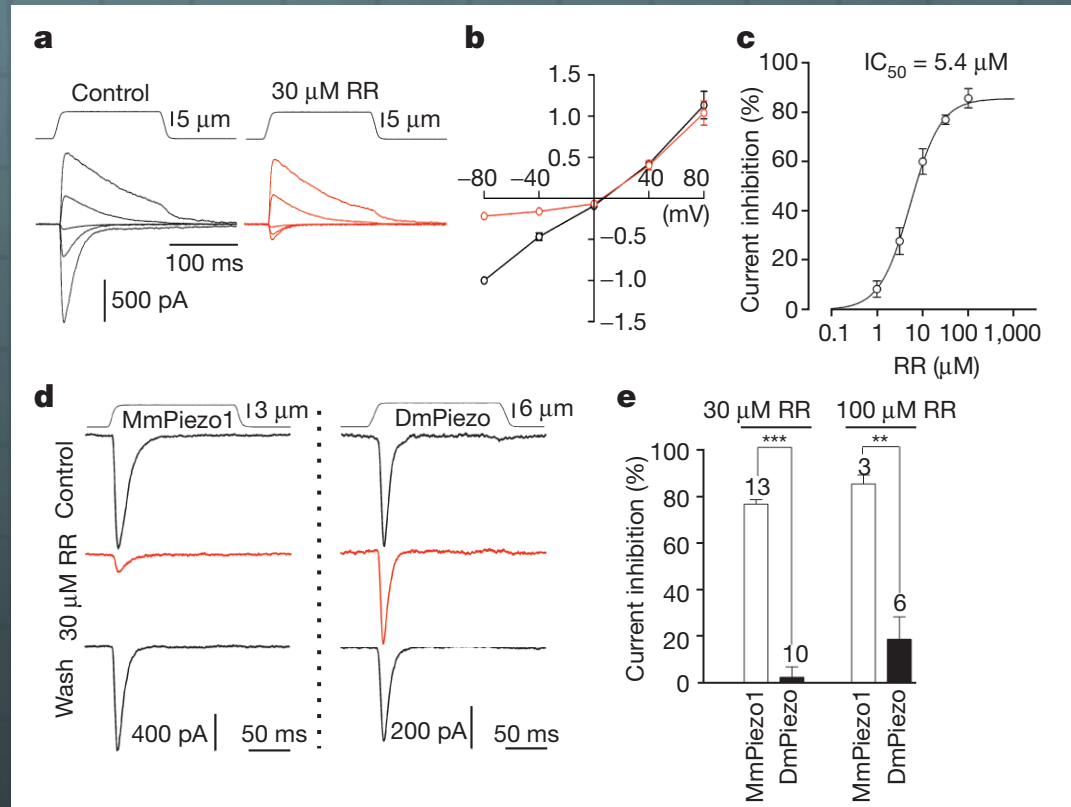


We further characterized DmPiezo-induced currents in HEK293T cells in response to negative pressure pulses applied through the recording pipette in the cell-attached mode, an alternative mechanosensitivity assay. Overexpression of DmPiezo induced stretch activated currents (Fig. 1d, e) with a pressure for half-maximal activation (P_{50}) of -31.8 mmHg (Fig. 1f), similar to the P_{50} calculated for MmPiezo1-induced currents (-30 mmHg).

Therefore, **mechanosensitivity of the Piezo family is conserved in invertebrates.**

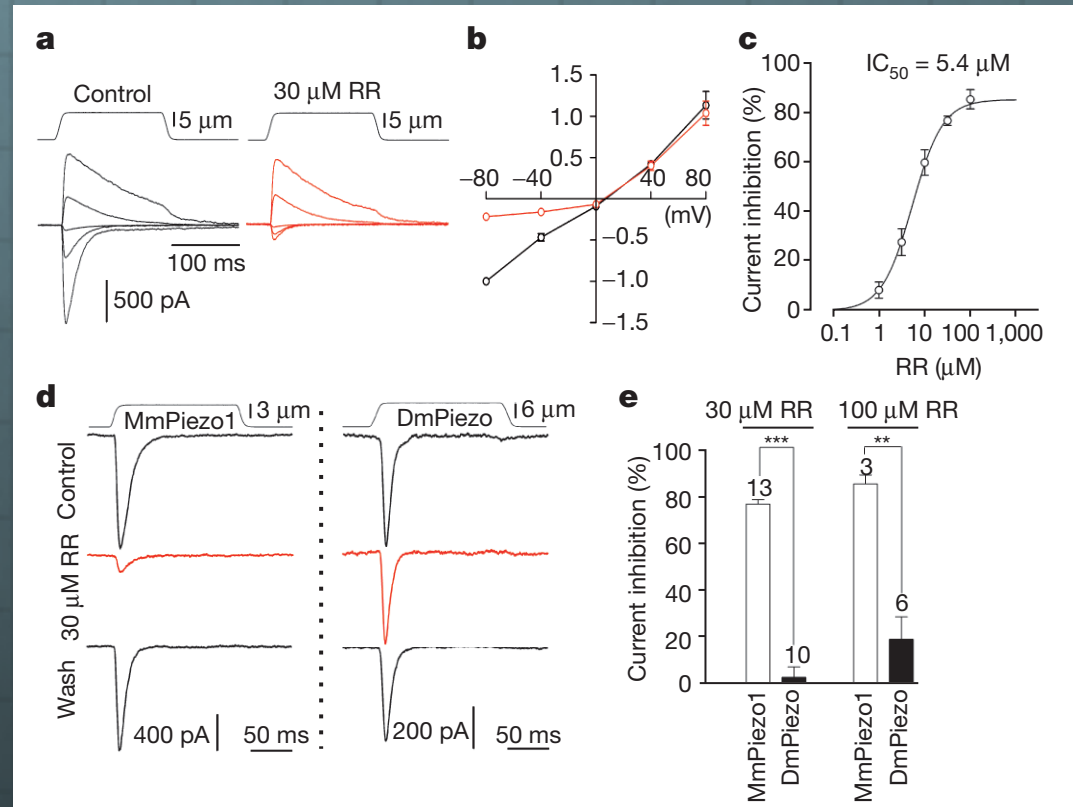
Pore properties of Piezo proteins

Ruthenium red, a polycationic pore blocker of TRP channels blocks **MmPiezo1** and **MmPiezo2**-induced mechanically activated currents. We found that ruthenium red is a voltage-dependent blocker of MmPiezo1, with an IC_{50} value of 5.460.9 μ M at -80mV (Fig. 2a–c): at a concentration of 30 μ M, extracellular ruthenium red inhibited inward mechanically activated currents without affecting outwards currents.



Pore properties of Piezo proteins

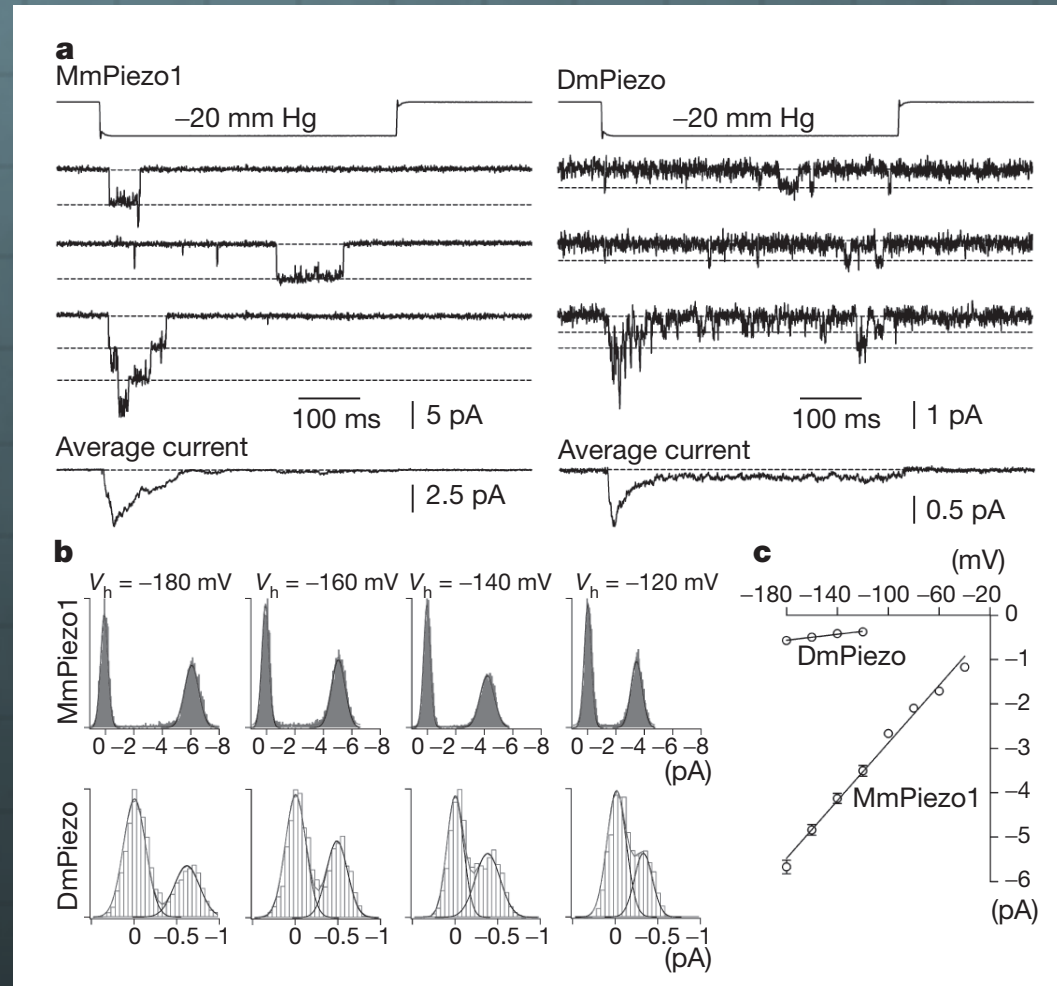
Notably, **DmPiezo** induced mechanically activated currents were **insensitive to ruthenium red** concentrations that potently blocked MmPiezo1-induced currents (Fig. 2d, e).



Together, these results demonstrate that overexpression of **DmPiezo** or **MmPiezo1** gives rise to mechanically activated channels with distinct channel properties.

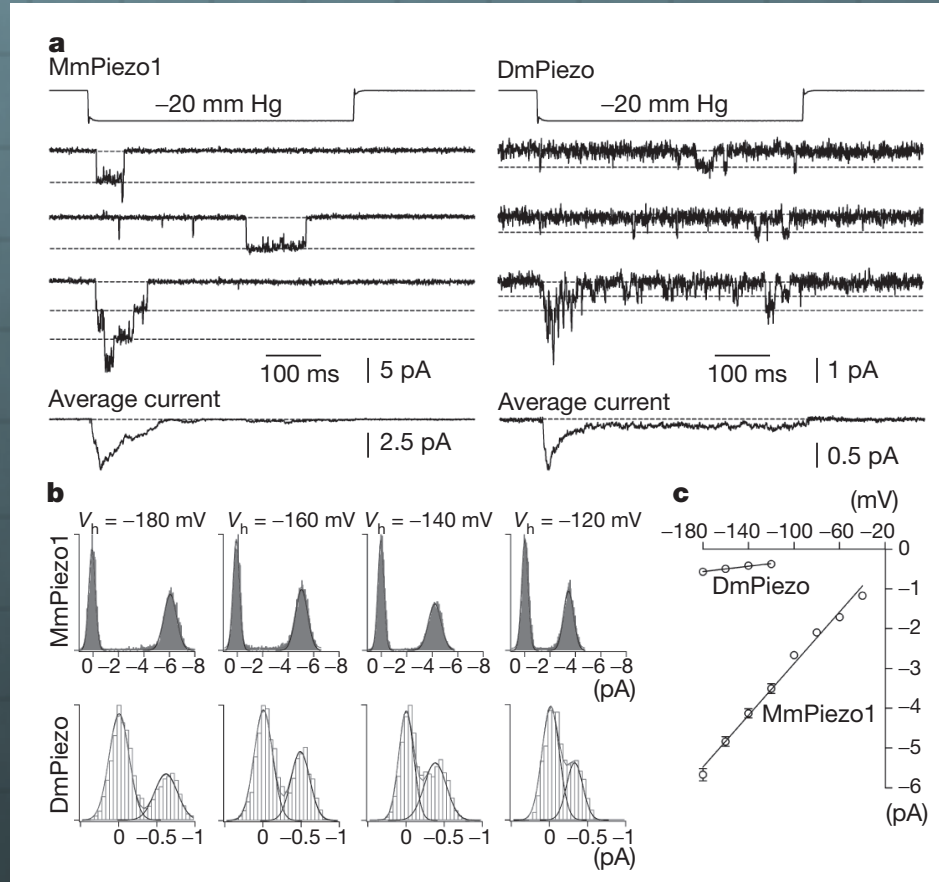
Pore properties of Piezo proteins

we set out to determine the single channel conductance (χ) of mechanically activated channels induced by Piezo proteins by using negative-pressure stimulations of membrane patches in cell-attached mode. Figure 3 shows the single mechanically activated channel properties of MmPiezo1 or DmPiezo




Pore properties of Piezo proteins

Openings of stretch-activated channels showed a marked difference in amplitude of single channel currents (Fig. 3a), as determined from the single channel I-V relationship for MmPiezo1 and DmPiezo (Fig. 3b, c).



DmPiezo-dependent channels are **nine fold less conductive** than **MmPiezo1**-dependent channels

 Mouse Piezo1 (MmPiezo1) and MmPiezo2 (also called Fam38a and Fam38b, respectively) induce mechanically activated cationic currents in cells; however, **it is unknown whether Piezo proteins are pore-forming ion channels or modulate ion channels**

00 MONTH 2012 | VOL 000 | NATURE | 1

ublishers Limited. All rights reserved.

ARTICLE

doi:10.1038/nature10812

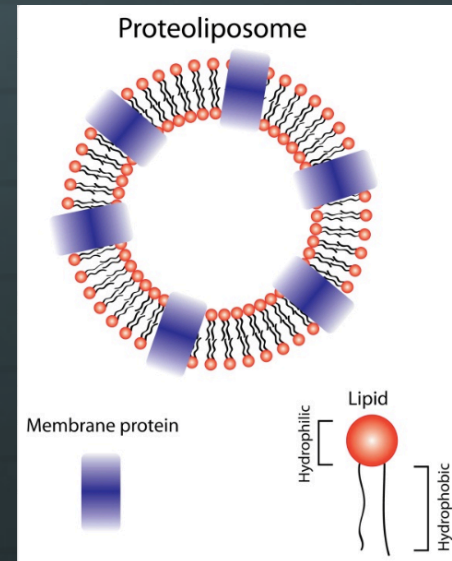
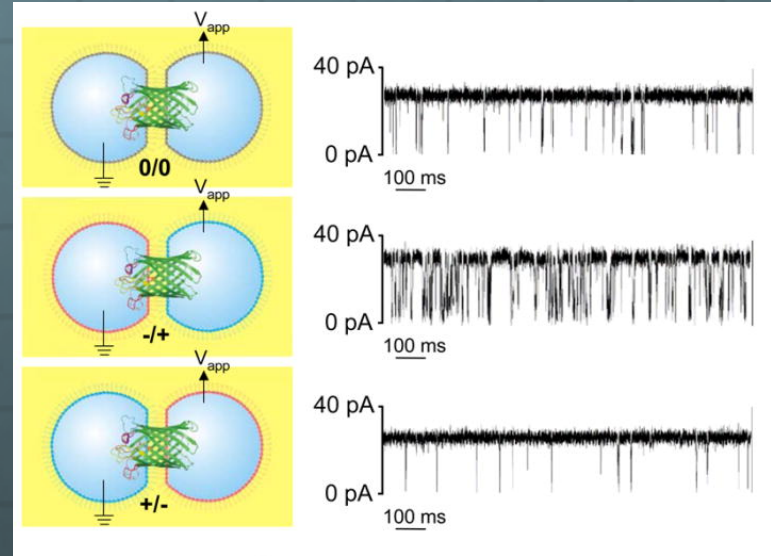
Piezo proteins are pore-forming subunits of mechanically activated channels

Bertrand Coste^{1*}, Bailong Xiao^{1*}, Jose S. Santos², Ruhma Syeda², Jörg Grandl^{1†}, Kathryn S. Spencer¹, Sung Eun Kim¹, Manuela Schmidt¹, Jayanti Mathur³, Adrienne E. Dubin¹, Mauricio Montal² & Ardem Patapoutian^{1,3}

MmPiezo1 reconstitution in lipid bilayers

to assess whether Piezo proteins were sufficient to recapitulate the channel properties recorded from Piezo-overexpressing cells, we reconstituted purified MmPiezo1 proteins into lipid bilayers in two distinct configurations: droplet interface lipid bilayers (DIBs) assembled from two monolayers (Fig. 5a–e and l–q) and proteoliposomes (Fig. 5f–h). In the first configuration, MmPiezo1 was reconstituted into asymmetric bilayers that mimic the cellular environment: the extracellular-facing lipid monolayer is predominantly neutral whereas the intracellular-facing leaflet is negatively charged. In contrast, the lipid composition of the bilayer in the second configuration is uniform.

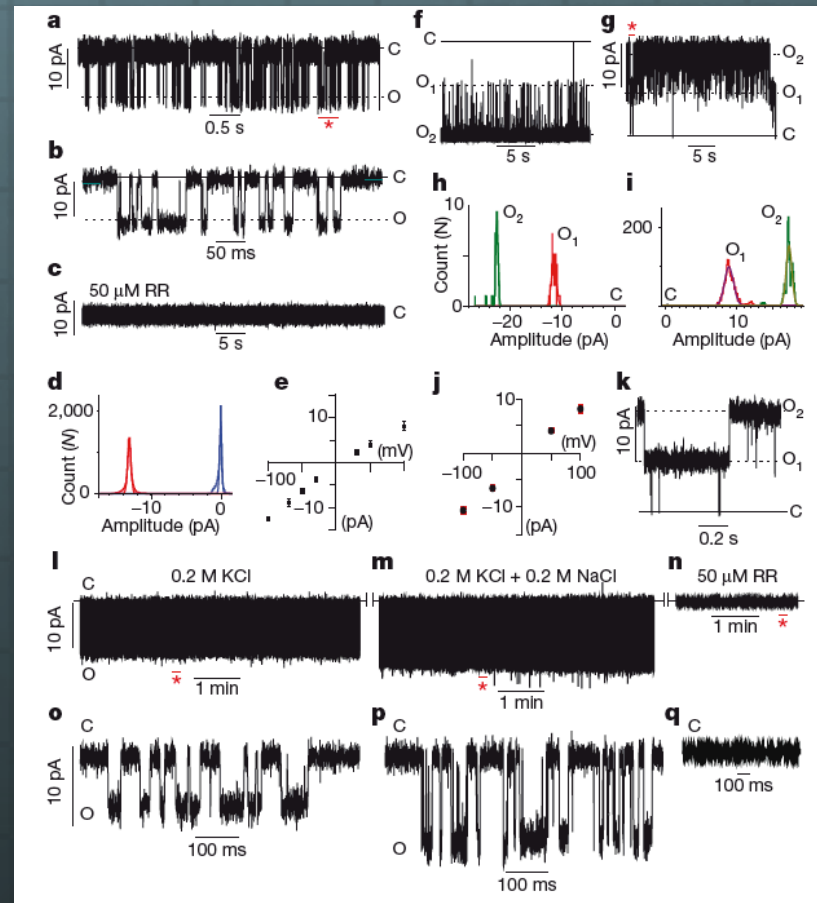
DIB



MmPiezo1 reconstitution in lipid bilayers

In the DIBs setting, representative segments from a 6-min recording obtained at -100mV show brief, discrete channel openings (Fig. 5a, b) blocked by addition of 50 μ M ruthenium red to the neutral facing compartment (Fig. 5c)

The asymmetric accessibility of ruthenium red block of reconstituted channels agrees with the data obtained from MmPiezo1-overexpressing HEK293T cells (Fig. 2 and), thereby establishing the fidelity of the assays and **validating MmPiezo1 protein as an authentic ion channel**



Architecture of the mammalian mechanosensitive Piezo1 channel

Jingpeng Ge^{1,2*}, Wanqiu Li^{2*}, Qiancheng Zhao^{1,3*}, Ningning Li^{2*}, Maofei Chen^{1,2}, Peng Zhi³, Ruochong Li^{1,2}, Ning Gao², Bailong Xiao^{1,3,4} & Maojun Yang^{1,2}

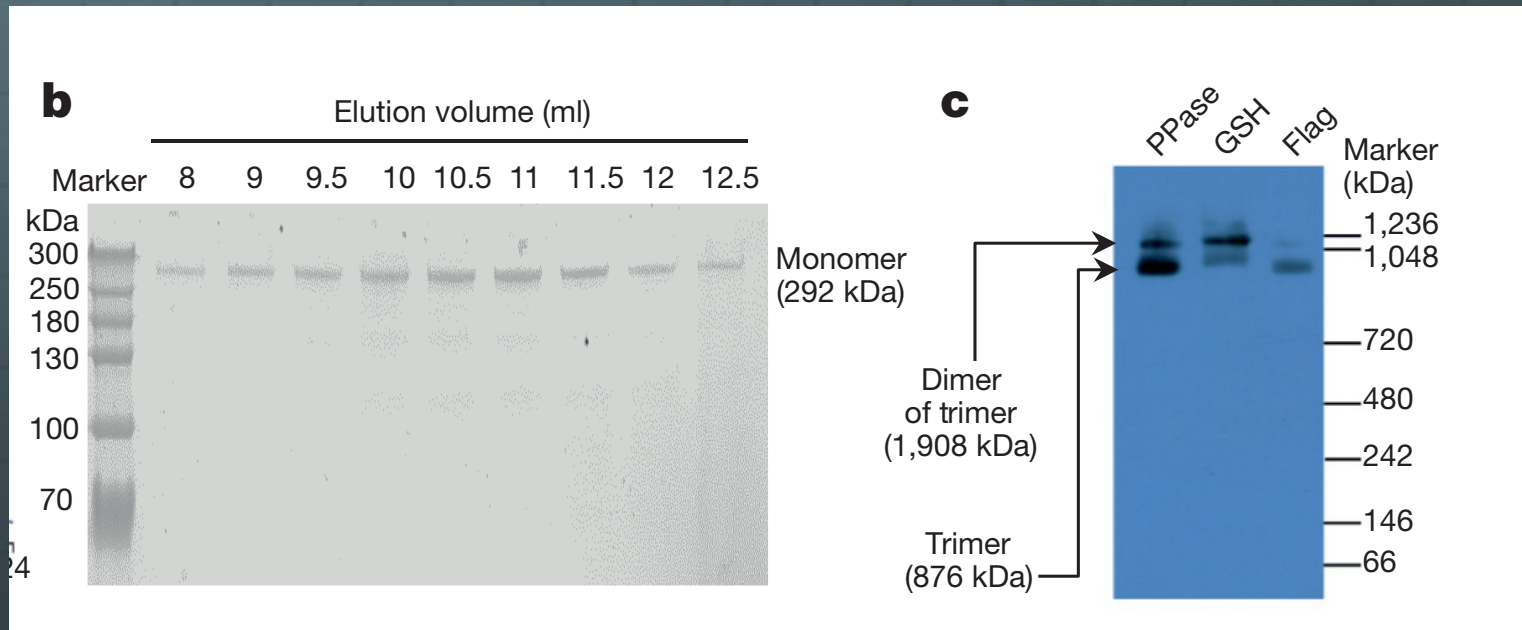
64 | NATURE | VOL 527 | 5 NOVEMBER 2015

©2015 Macmillan Publishers Limited. All rights reserved

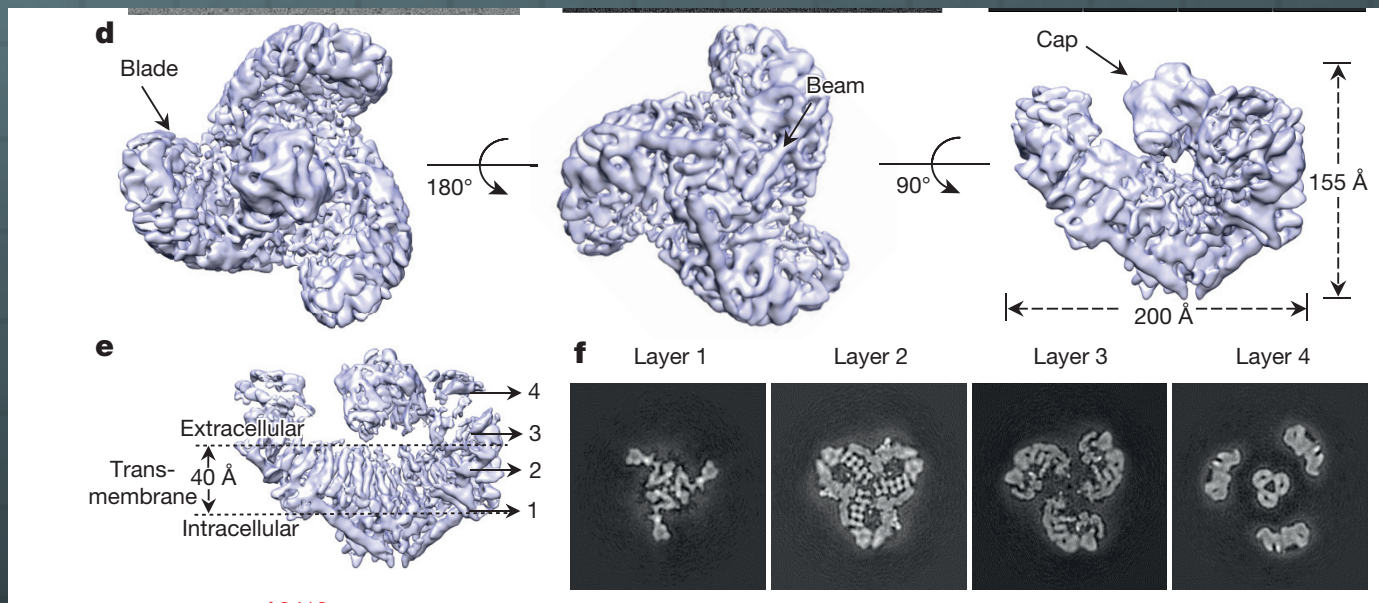
Here we determine the cryo-electron microscopy structure of the full-length (2,547 amino acids) mouse Piezo1 (Piezo1) at a resolution of 4.8 Å .

Piezo1 forms a trimeric propeller-like structure (about 900 kilodalton), with the extracellular domains resembling three distal blades and a central cap.

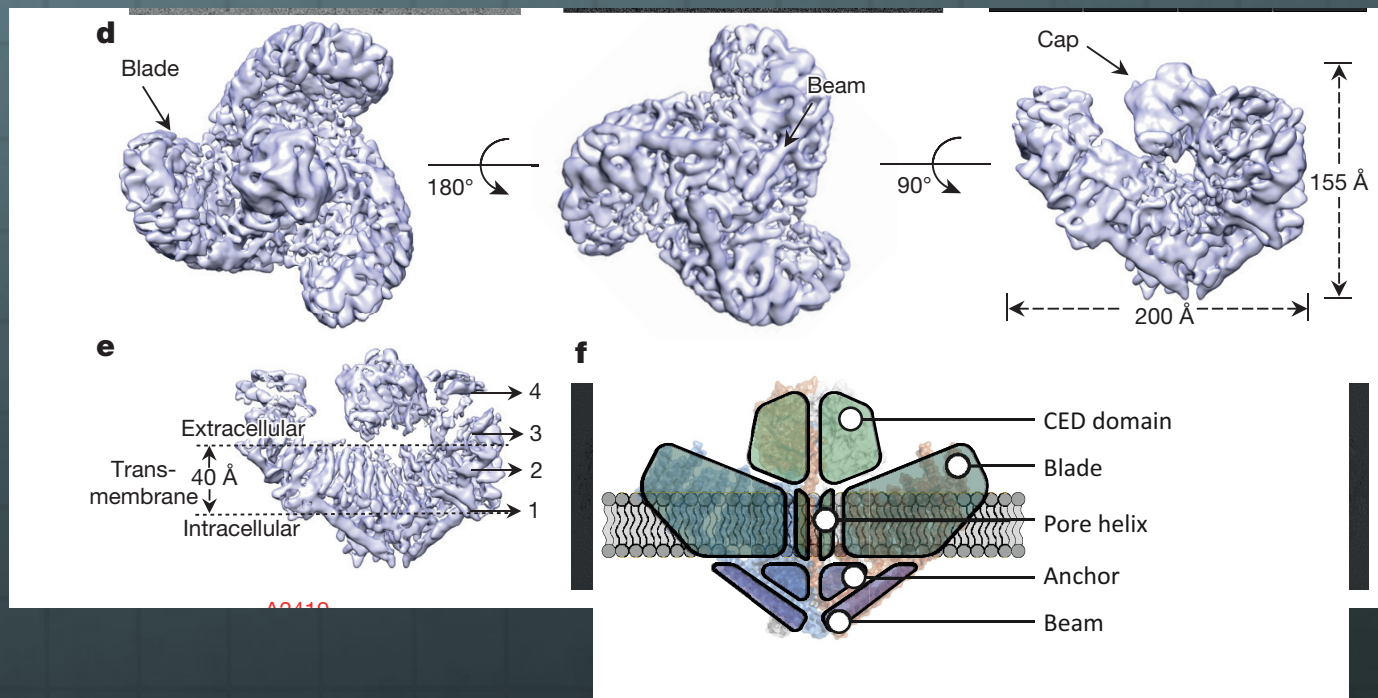
As a further confirmation, Flag-tagged Piezo1 displayed a major band at about 900 kDa on native gels (Fig. 1c). Thus, our data suggest that the major oligomeric state of the purified Piezo1 is trimeric.



The density map revealed that Piezo1 formed a three-blade, propeller-shaped architecture, with distinct regions resembling the typical structural components of a propeller, including three blades and a central cap. Viewed from the top, the diameter and the axial height of the structure are 200 Å and 155 Å, respectively (Fig. 2d).



A single central cap sits above the surface of the transmembrane core with a gap in between (Fig. 2e). Furthermore, a tightly packed region, likely to be a compact soluble domain, is located on the opposite side of the cap, right below the transmembrane region (Fig. 2e). The anchor, which may contain the highly conserved PF(X2)E(X6)W motif found in Piezos in all species, also results in clockwise swapping of the OH and CED of one monomer into the region of the neighboring monomer (Figure 4).

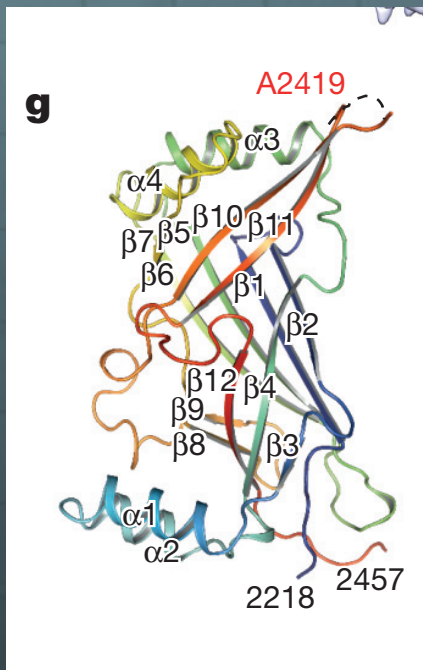


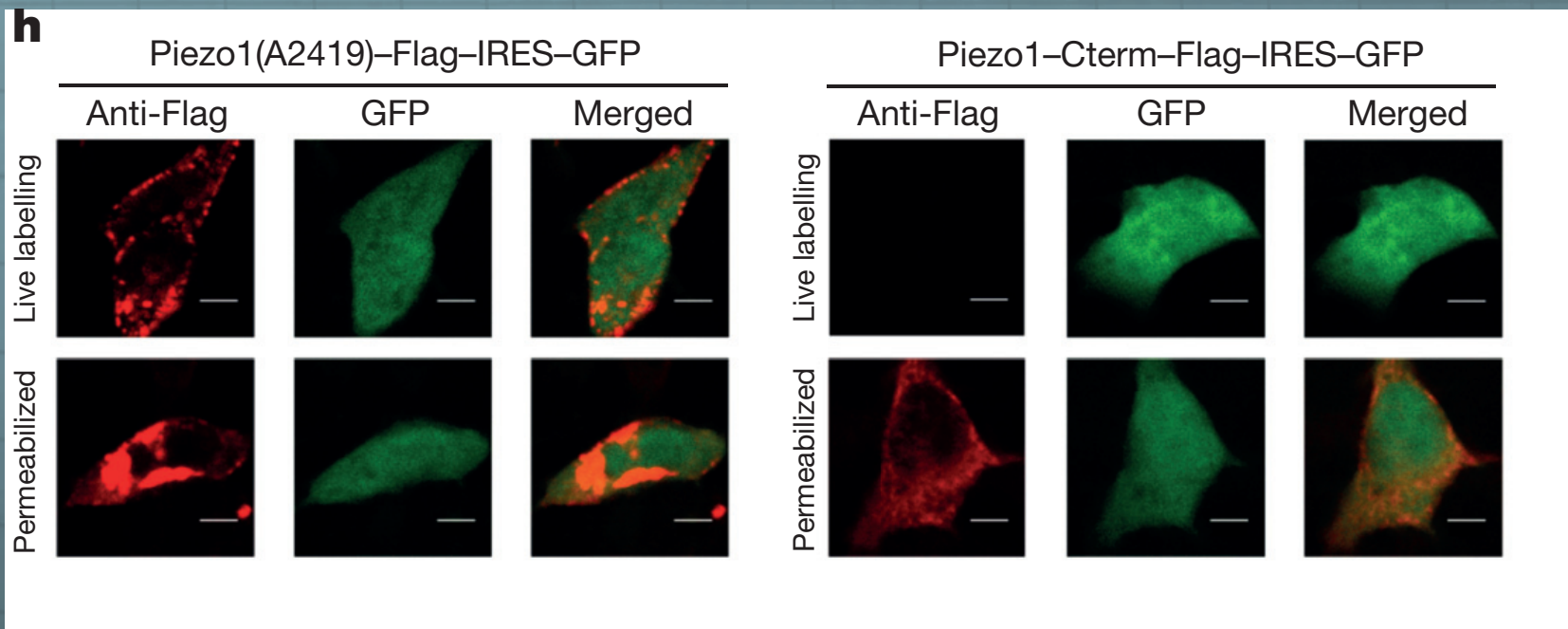
The Cap is constituted by residues from 2210 to 2457 (termed the C-terminal extracellular domain, CED) that form a large extracellular loop followed by the last transmembrane segment at the C terminus.

CRISTAL STRUCTURE OF CED:

The amino (N) and C termini of the CED are on the same side and close to each other (Fig. 2g), consistent with the topological prediction that the CED is located between the last two transmembrane segments **in the C-terminal region of Piezo1**.

In the 3D structure, the CAP is formed by a CED trimer, further supporting the conclusion that the full-length Piezo1 forms a homotrimer.

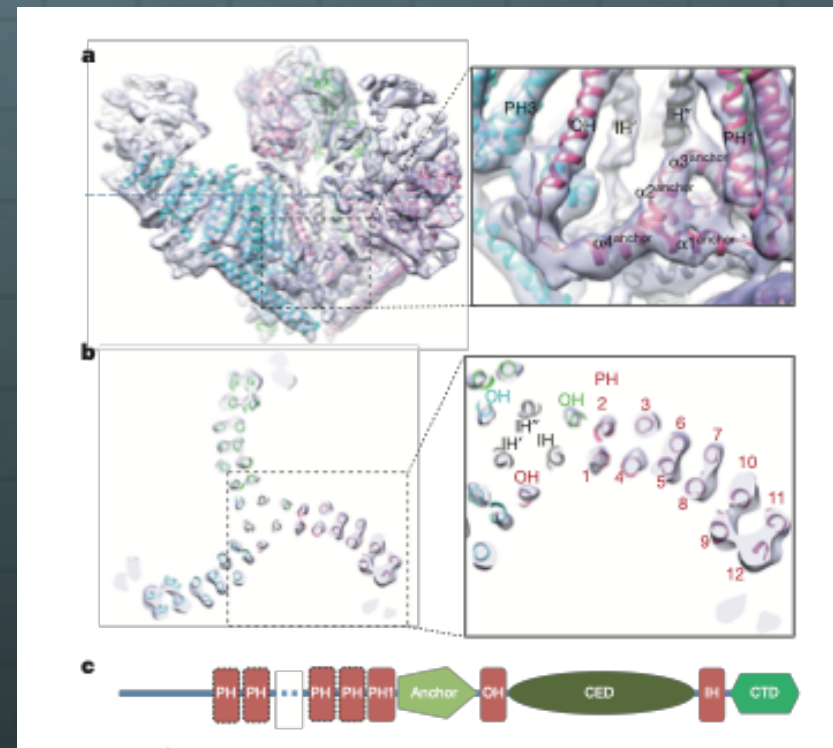




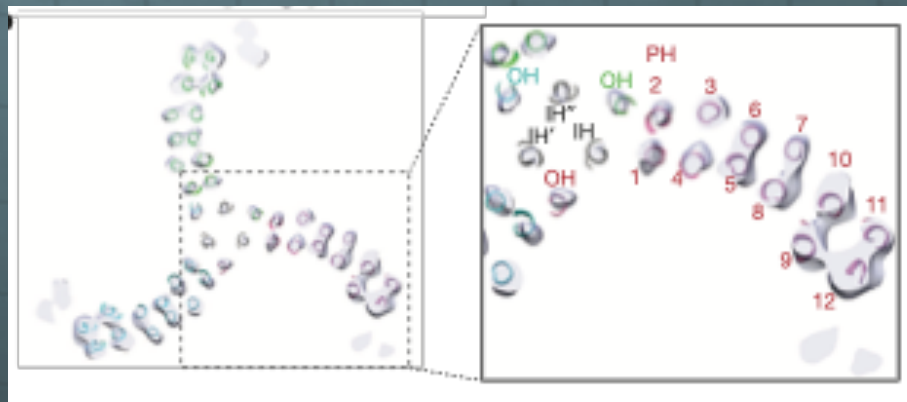
To further confirm the topological location of the CED and the C terminus of Piezo1, we performed immunolabelling of live HEK293T cells expressing Piezo1 with a Flag tag fused either in a flexible loop of the CED (after A2419) or at the C terminus of Piezo1. Using confocal microscopy, we found that the Flag tag could be labelled on the plasma membrane of live cells only when inserted in the CED and not at the C terminus (Fig. 2h). **These data demonstrate that the CED is an extracellular domain, whereas the C terminus is intracellular, consistent with a recent report**

The transmembrane region has 14 apparently resolved segments per subunit. These segments form three peripheral wings and a central pore module that encloses a potential ion-conducting pore. The rather flexible extracellular blade domains are connected to the central intracellular domain by three long beam-like structures.

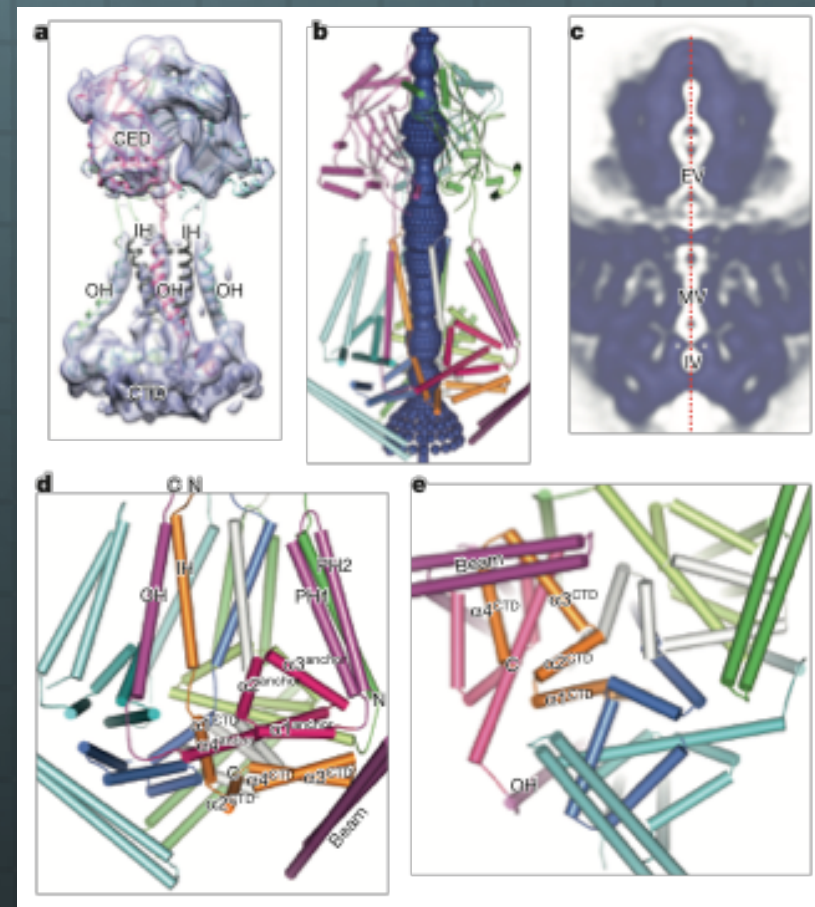
We refer to the core transmembrane segments as inner helix (IH) and outer helix (OH) and to the peripheral trans-membrane arrays as peripheral helix (PH) (Fig. 3). The 12 PHs from the same monomer are organized as six helical pairs, extending from the central axis to the periphery of the complex (Fig. 3b).



The centre of the Piezo1 channel within the membrane consists of **six transmembrane helices** in a triangular arrangement (Fig. 3b, right and Fig. 4). Three IHs, presumably extended from the C termini of the CEDs, are located at the innermost position and seem to line a central pore. Three OHs, extended from the N termini of the CEDs, further enclose the three IHs (Fig. 4a).

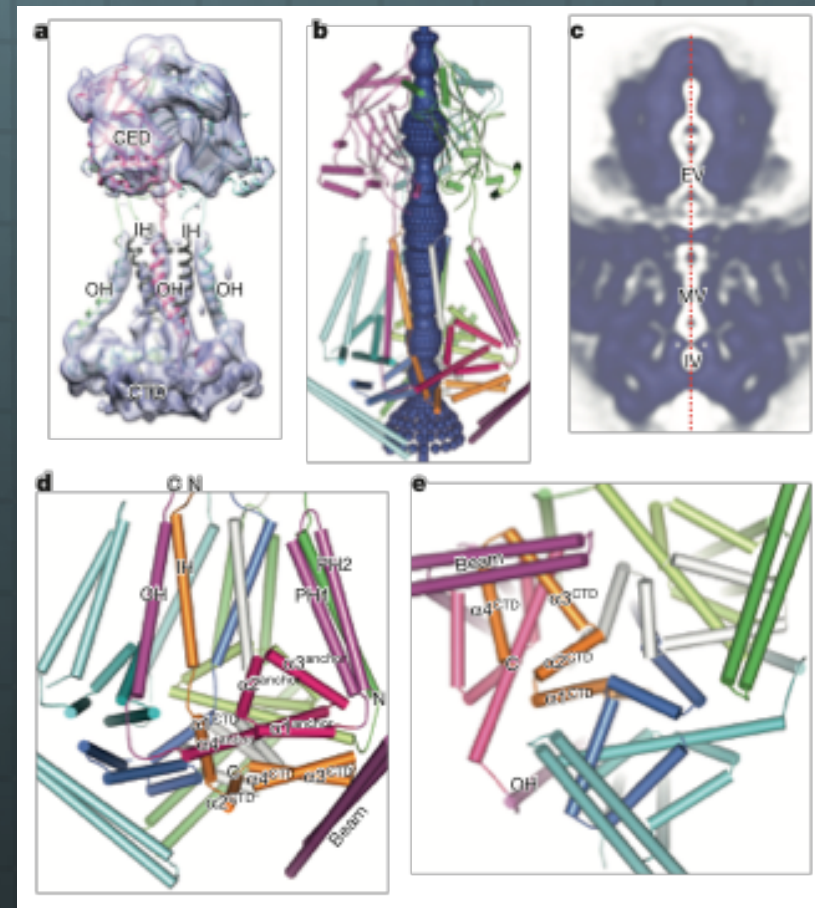


This central region, including the IH– OH pairs, the CEDs and the CTDs, probably comprises the pore module of Piezo1.

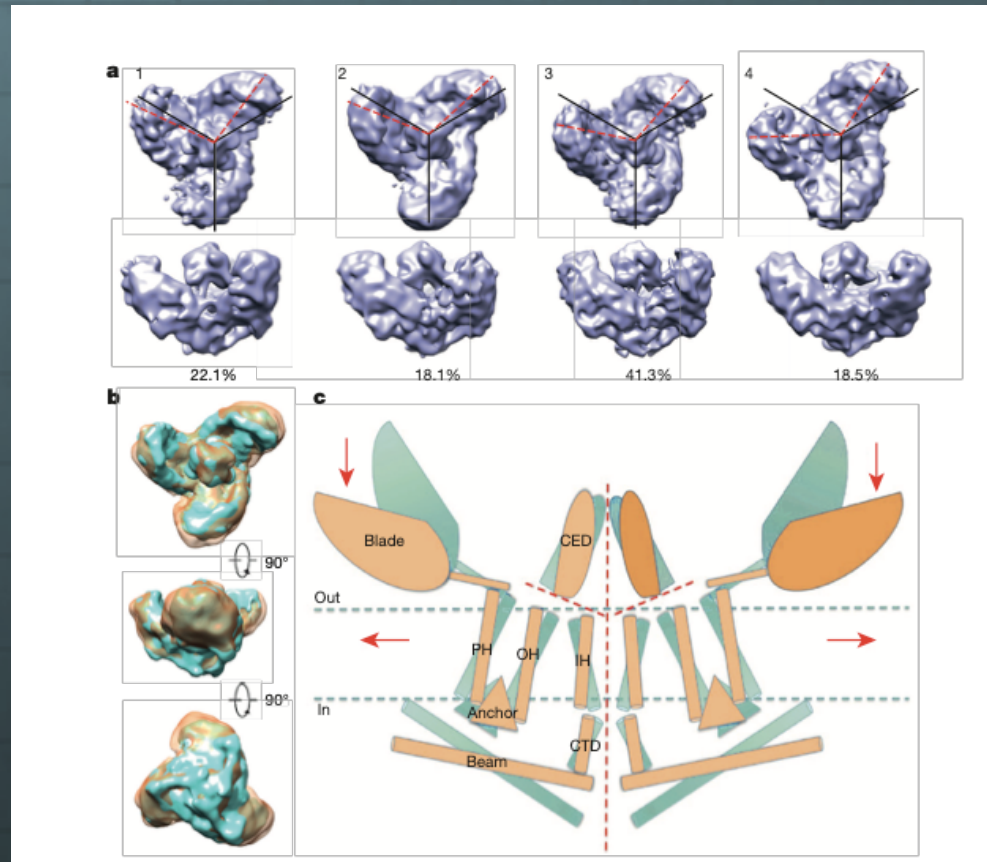


The central slice of the rotationally averaged density map revealed a continuous central channel along the z-axis, including an extracellular vestibule within the cap, a transmembrane vestibule enclosed by the three IHs and an intracellular vestibule formed by the trimeric CTD (Fig. 4b–e).

Based on this structural information, we propose that the OH–CED–IH–CTD-containing region functions as the pore module of Piezo channels (Fig. 4).



The most notable one is that the rotational spacing between two adjacent blades varies from 100° to 140° (Fig. 5a). Other less pronounced but identifiable conformational variations include the tilting of the blade relative to the plasma membrane and curvature changes on the helicoidal surface (Fig. 5b).



ACTIVATION MECHANISMS

- Mechanical force can be directly transmitted to the channel through lateral tension in the membrane bilayer, whereby the conformation with the greater cross-sectional area is favored under higher tension. For Piezo1, both the cap and the first two extracellular loops near the N terminus are mechanically sensitive, as pulling on them with magnetic force induces changes in channel activation and inactivation. The curvature and large size of the peripheral blades may position them as particularly efficient sensors of membrane geometry.
- The coupling of mechanical energy to pore opening could also be mediated by interactions of a membrane lipid with a binding pocket on the protein, as has been established for the mechanosensitive channels TRAAK and MscS. Depleting phosphoinositides, including phosphatidylinositol 4,5-bisphosphate (PIP₂), from the patch membrane inhibits Piezo1 and Piezo2 activity, indicating that a similar mechanism could contribute to Piezo gating

ACTIVATION MECHANISMS

- Piezo activity can also be titrated by a diverse array of modulators, which can be broadly divided into two categories:
 - those acting on membrane properties, and thus indirectly modulating channel function, and
 - those acting through direct interactions with the channel itself.

Notably, the precise mechanism (passive vs. active) has not yet been elucidated for many modulators, some of which could in theory act either on the channel or on the membrane.